III-V-on-silicon multi-frequency lasers

III-V-on-silicon multi-frequency lasers

S. Keyvaninia,[1,2,*] S. Verstuyft,[1,2] S. Pathak,[1,2]
F. Lelarge,[3] G.-H. Duan,[3] D. Bordel,[4] J.-M. Fedeli,[4] T. De Vries,[5] B. Smalbrugge,[5]
E. J. Geluk,[5] J. Bolk,[5] M. Smit,[5] G. Roelkens,[1,2] and D. Van Thourhout[1,2]

[1]*Photonics Research Group, Ghent University-imec, Sint-Pietersnieuwstraat 41, B-9000 Ghent, Belgium*
[2]*Center for Nano- and Biophotonics (NB-Photonics), Ghent University, Ghent, Belgium*
[3]*III-V lab, III-V Lab, a joint lab of 'Alcatel-Lucent Bell Labs France', 'Thales Research and Technology' and 'CEA Leti', Campus Polytechnique, 1, Avenue A. Fresnel, 91767 Palaiseau cedex, France*
[4]*CEA, LETI, Minatec 17 Rue des Martyrs Grenoble France*
[5] *Photonic Integration Group, Eindhoven University of Technology, Den Dolech 2, Eindhoven, The Netherlands*
[*]*shahram.keyvaninia@intec.ugent.be*

Abstract: Compact multi-frequency lasers are realized by combining III-V based optical amplifiers with silicon waveguide optical demultiplexers using a heterogeneous integration process based on adhesive wafer bonding. Both devices using arrayed waveguide grating routers as well as devices using ring resonators as the demultiplexer showed lasing with threshold currents between 30 and 40 mA and output powers in the order of a few mW. Laser operation up to 60°C is demonstrated. The small bending radius allowable for the silicon waveguides results in a short cavity length, ensuring stable lasing in a single longitudinal mode, even with relaxed values for the intra-cavity filter bandwidths.

OCIS codes: (250.0250) Optoelectronics; (250.5300) Photonic integrated circuits; (250.5960) Semiconductor lasers.

References and links

1. R. Monnard, C. R. Doerr, C. H. Joyner, M. Zirngibl, and L. W. Stulz, "Direct modulation of a multifrequency laser up to 16 x 622 Mb/s," IEEE Photon. Technol. Lett. **9**(6), 815–817 (1997).
2. C. R. Doerr, C. H. Joyner, and L. W. Stulz, "40-wavelength rapidly digitally tunable laser," IEEE Photon. Technol. Lett. **11**(11), 1348–1350 (1999).
3. K. Lawniczuk, I. G. Knight, P. J. Williams, M. J. Wale, R. Piramidowicz, P. Szczepanski, M. K. Smit, and X. J. M. Leijtens, "Multiwavelength photonic transmitters in a multi-project wafer run" in Proceedings Symposium IEEE Photonics Society Benelux, 2011, Ghent, Belgium (2011), 173–176.
4. G. Kurczveil, M. J. Heck, J. D. Peters, J. M. Garcia, D. Spencer, and J. E. Bowers, "An integrated hybrid silicon multiwavelength AWG laser," IEEE J. Sel. Top. Quantum Electron. **17**(6), 1521–1527 (2011).
5. S. Keyvaninia, G. Roelkens, D. Van Thourhout, C. Jany, M. Lamponi, A. Le Liepvre, F. Lelarge, D. Make, G.-H. Duan, D. Bordel, and J.-M. Fedeli, "Demonstration of a heterogeneously integrated III-V/SOI single wavelength tunable laser," Opt. Express **21**(3), 3784–3792 (2013).
6. M. Lamponi, S. Keyvaninia, C. Jany, F. Poingt, F. Lelarge, G. De Valicourt, G. Roelkens, D. Van Thourhout, S. Messaoudene, J. Fedeli, G. H. Duan, and S. Member, "Low-threshold heterogeneously integrated InP / SOI lasers with a double adiabatic taper coupler," IEEE Photon. Technol. Lett. **24**(1), 76–78 (2012).
7. W. Bogaerts, S. Selvaraja, P. Dumon, J. Brouckaert, K. De Vos, D. Van Thourhout, and R. Baets, "Silicon-on-insulator spectral filters fabricated with CMOS technology," IEEE J. Sel. Top. Quantum Electron. **16**(1), 33–44 (2010).
8. C. R. Doerr, M. Zirngibl, and C. H. Joyner, "Single longitudinal-mode stability via wave mixing in long-cavity semiconductor lasers," IEEE Photon. Technol. Lett. **7**(9), 962–964 (1995).
9. C. Doerr, C. Joyner, M. Zirngibl, and L. W. Stulz, "Chirped waveguide grating router multifrequency laser with absolute wavelength control," IEEE Photon. Technol. Lett. **8**(12), 1606–1608 (1996).
10. F. Van Laere, T. Claes, J. Schrauwen, S. Scheerlinck, W. Bogaerts, D. Taillaert, L. O'Faolain, D. Van Thourhout, and R. Baets, "Compact focusing grating couplers for silicon-on-insulator integrated circuits," IEEE Photon. Technol. Lett. **19**(23), 1919–1921 (2007).
11. S. Keyvaninia, M. Muneeb, S. Stanković, P. J. Van Veldhoven, D. Van Thourhout, and G. Roelkens, "Ultra-thin DVS-BCB adhesive bonding of III-V wafers, dies and multiple dies to a patterned silicon-on-insulator substrate," Opt. Mater. Express **3**(1), 35–46 (2013).
12. D. Derrickson, *Fiber Optic Test and Measurement* (Prentice Hall, 1998), pp. 185.

#187534 - $15.00 USD Received 21 Mar 2013; revised 6 May 2013; accepted 7 May 2013; published 30 May 2013

1. Introduction

Multi-frequency lasers (MFL) are attractive devices for use in high-capacity WDM networks [1] or as digitally tunable lasers [2]. They can be realized by integrating a semiconductor amplifier array and a wavelength demultiplexer within a laser cavity as schematically shown in Fig. 1(a). The optical demultiplexer filters the amplified spontaneous emission (ASE) coming from the amplifier and if the gain provided is sufficient to overcome the intra-cavity losses and the mirror losses, the device will start lasing at the wavelengths determined by the demultiplexer. Such devices fully integrated on an InP based platform were intensively studied by e.g. Joyner, Doerr et al. at Bell Labs, using an arrayed waveguide grating (AWG) as the demultiplexer. The best of these devices had a threshold current of 18-30 mA and a fiber coupled output power of slightly over 1mW [3]. Devices with 16 and more channels were demonstrated [1]. More recently Ławniczuk et al. [3] demonstrated a 4-channel device integrated in a generic InP-based photonic IC process. This device had a somewhat higher threshold current but was integrated with on-chip modulators. Kurczveil et al. demonstrated a 4-channel MFL using a hybrid integration process whereby InP-silicon evanescently coupled amplifiers and a silicon-based AWG were integrated using a wafer-bonding process [4]. While this showed for the first time the potential of such a process, the performance was limited by the relatively low gain of the amplifiers and a high loss in the passive sections, resulting in a threshold current of over 100 mA.

All of the devices reported above had a relatively long cavity length (6-10 mm), mainly determined by the size of the passive demultiplexer. This limits the direct modulation speed of the devices [1] as well as their switching speed [2]. We recently demonstrated a heterogeneous integration platform consisting of InP-based amplifiers adiabatically coupled with nano-photonic silicon waveguide devices fabricated in a 400 nm/220 nm SOI-layer (Silicon-On-Insulator) [5,6]. This allows for the realization of very compact filter devices, such as ring resonators and AWG demultiplexers [7]. Using this platform we are able to realize much more compact multi-frequency lasers, as we demonstrate in this paper. Furthermore the performance of our devices comes close to that of the best multi-frequency lasers demonstrated so far. Below we will first elaborate on the design of our devices. Next we will discuss the fabrication process. Finally, in section 4 we discuss the characterization results in depth.

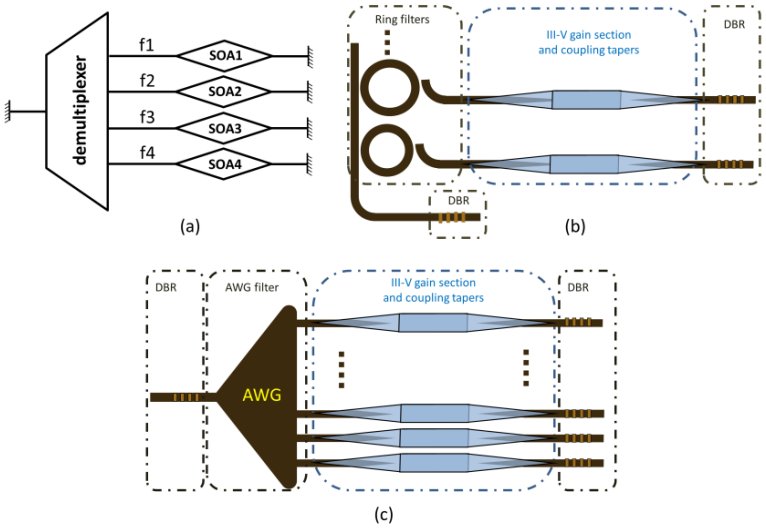

Fig. 1. a) Schematic structure of a multi-frequency laser; b) Heterogeneous III-V/silicon MFL based on ring resonator demux; c) Heterogeneous III-V/silicon MFL based on AWG demux.

#187534 - $15.00 USD Received 21 Mar 2013; revised 6 May 2013; accepted 7 May 2013; published 30 May 2013

2. Device design

2.1 Overview

Figure 2(a) shows a microscope picture of a chip containing two multi-frequency lasers using a ring resonator based demultiplexer (RMFL) and one multi-frequency laser based on an AWG demultiplexer (AMFL), each with 4 wavelength channels. It is immediately obvious that the chip space is no longer fully dominated by the passive demultiplexer, as was the case with earlier MFL devices, but rather by the amplifier array. Figure 1(b) and Fig. 2(b) show the structure of the RMFL in more detail. It consists of 4 semiconductor optical amplifiers (SOA), connected to a 4-channel ring demultiplexer. The laser cavity is formed by highly reflective DBR mirrors at the right side of each of the amplifiers – denoted as "back DBR" in Fig. 2(b) – and a DBR mirror with lower reflectivity at the common output port of the ring based demultiplexer – denoted as "front DBR" in Fig. 2(b). Light exiting from this side is guided through a silicon waveguide towards a fiber-to-chip grating coupler at the right side of the device, where light is coupled out vertically towards a single mode fiber. The AMFL, shown in Fig. 1(c) and Fig. 2(a) has a similar structure with four SOAs connected to the input side of the AWG and a common DBR mirror (back DBR) at the output side of the AWG. In this case light is coupled out through the front DBR mirrors and grating couplers connected to the SOA side of the device (left side of Fig. 2(a)).

2.2 Amplifiers

The amplifiers are defined in an InP-epitaxial layer stack integrated on top of the silicon waveguides using an adhesive bonding process (see section 3 for details on the fabrication process). The bonding layer thickness was 110 nm in this case. The semiconductor layer stack consists of a p-InGaAs contact layer, a p-InP cladding layer (1.5 μm thick), six InGaAsP quantum wells (6 nm) surrounded by two InGaAsP separate confinement heterostructure layers (100 nm thick, bandgap wavelength 1.17 μm) and a 200 nm thick n-type InP layer. The amplifiers are 500 μm long and 3 μm wide and initially taper down to 900 nm over a length of 45 μm on both sides. They are separated from each other by 50 μm. The amplifier mesa was defined by etching down to the n-type contact layer. Light is coupled from the SOAs to the underlying silicon waveguides using a 150 μm long adiabatic taper. To maximize the coupling efficiency both the III-V waveguide and the silicon waveguide are tapered. The silicon ridge waveguide is defined in a 400 nm thick silicon layer and etched 180 nm deep. The III-V/silicon taper structure consists of two sections: the III-V mesa is gradually tapered from 900 nm to 500 nm over a length of 150 μm while at the same time the silicon ridge waveguide underneath tapers from 300 nm to 1 μm. At the end of this section all the light is now confined to the 400 nm thick silicon ridge waveguide. Finally this waveguide is coupled to a 220 nm high strip waveguide using a short adiabatic taper structure.

2.3 Passive demultiplexer

The passive optical demultiplexer circuits needed for the MFL were formed in the 220 nm thick silicon device layer, using 450 nm wide silicon strip waveguides. These are single mode and allow for a bend radius of less than 3 μm, leading to very compact circuits. The most important parameters in designing a demultiplexer for a MFL are its free spectral range (FSR) and the relation between longitudinal mode spacing and filter bandwidth. The FSR should be large enough to guarantee stable lasing in only one passband. The filter bandwidth should be sufficiently small compared to the longitudinal mode spacing to guarantee suppression of neighboring longitudinal modes.

The ring-based demultiplexer circuit (Fig. 2(c)) consists of four ring resonators coupled to a common bus waveguide. The radius of the first ring resonator is 4.98 μm and has a 1 μm racetrack length, resulting in a free spectral range of 15.5 nm. The radius of the successive

#187534 - $15.00 USD Received 21 Mar 2013; revised 6 May 2013; accepted 7 May 2013; published 30 May 2013

ring resonators was gradually increased by 15 nm each, resulting in a targeted channel separation of 250 GHz. The gap between ring resonators and bus waveguides was fixed at 200 nm. From past experimental results on passive devices, we know this should result in a loaded quality factor of at least 3000 or a 3dB bandwidth of less than 65 GHz for the resonators. The total cavity length for the laser varies from channel to channel but is in worst case approximately 1700 μm, which, together with an estimated average group index of 3.95, leads to an estimated longitudinal mode spacing of 22 GHz. Therefore, longitudinal modes close to the lasing mode will have a round trip gain, which is at least a few dB lower than that for the lasing mode.

The AWG, visible in the top right corner of Fig. 2(a) was designed according to the procedure described in [6]. To reduce back reflections and losses the waveguides around the star couplers are shallowly etched (70 nm deep). The AWG footprint is approximately 400 μm by 700 μm. The designed channel spacing was 200 GHz, with a 3 dB bandwidth of 80 GHz. The FSR was designed to be 35 nm. The total cavity length for the AMFL is around 2.4 mm, leading to a longitudinal mode spacing of 15.6 GHz, assuming an average group index of 4.03. Hence at least 4 modes fit within the 3 dB bandwidth of the intra-cavity filter. However, it has been shown in the past that, despite the limited gain suppression between the different longitudinal modes, through four-wave mixing stable single mode lasing can be obtained in this kind of devices [8].

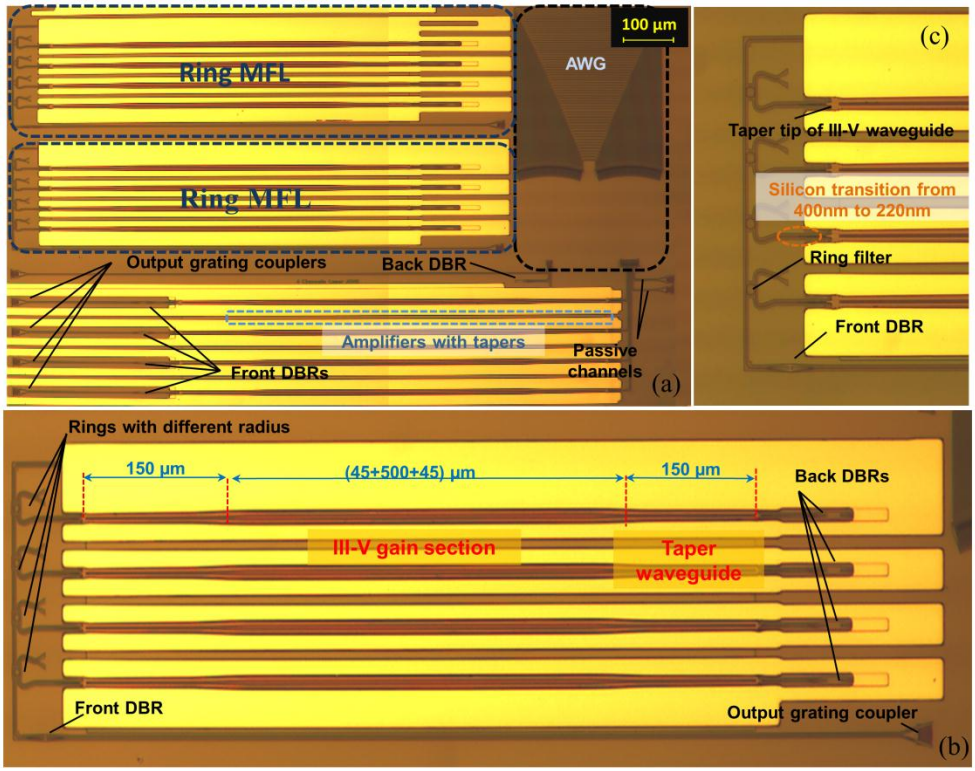

Fig. 2. Microscope picture of fabricated devices: a) overview picture showing two 4-channel ring MFL and a 4-channel AWG MFL; b) 4-channel ring MFL; c) Detail of ring demultiplexer.

2.3 DBR-mirrors and grating coupler

In a typical MFL, the laser cavity is formed by the cleaved facets of the semiconductor chip on which it is built. The high resolution patterning capabilities of our silicon waveguide platform provide a lot more flexibility. Here we implemented the reflectors as distributed

#187534 - $15.00 USD Received 21 Mar 2013; revised 6 May 2013; accepted 7 May 2013; published 30 May 2013

Bragg reflectors (DBR). This allows tailoring their strength lithographically, avoiding the need for dedicated facet coating processes, and to keep the light on the chip, which could be important for further processing. Although this feature was not used here, in principle it would also be possible to tailor the bandwidth of the DBR-mirrors such that they can help in suppressing lasing in higher or lower passbands of the demultiplexer and avoiding the need for special designs such as chirping the AWG passbands, which introduces extra losses [9]. The DBR-mirrors used here were etched on the surface on the silicon waveguide layer, using a 290 nm grating period, 70 nm etch depth and 50% duty cycle. The high reflectivity mirror consists of 40 grating periods (resulting in a reflectivity > 90% and a 3 dB bandwidth of 100 nm), while the partially reflecting mirror consists of 8 periods, resulting in 45% maximum reflection and a 3 dB bandwidth of 140 nm. More details on the grating design and characterization can be found in [4].

For coupling light out of the chip we used a focusing grating coupler [10], as visible in the bottom right corner of Fig. 2(b). These gratings were defined using the same 70 nm etch depth in the 220 nm device layer, which was also used for the DBR mirrors and the AWG star couplers (grating period 625 nm, 10 degree fiber angle). The estimated coupling loss is 5 dB (to cleaved single mode fiber) at a wavelength of 1550 nm.

3. Fabrication

The general fabrication flow of our heterogeneous III-V-on-silicon integration process was discussed in detail before [4,5]. First the silicon waveguides are fabricated, in this case starting from an SOI wafer with a 400 nm thick silicon waveguide layer. All patterns were defined using 193 nm deep UV lithography. A 180 nm deep etch step defines the 400 nm ridge waveguides and the 220 nm device layer, which is used for the passive silicon circuitry. Then a 70 nm deep etch step defines the DBR-mirrors and the grating couplers. In a last step the 220 nm strip waveguide are etched. Next, a SiO2 cladding layer is deposited and the wafer is planarized using chemical mechanical polishing (CMP) and a controlled wet etch down to the top of the 400 nm thick silicon waveguide layer.

The III-V epitaxial layer structure was grown on an InP substrate using MOCVD. It was bonded upside down onto the silicon waveguide layer using the process described in [11], resulting in a 110 nm thick intermediate DVS-BCB layer. Next the InP substrate was removed by wet chemical etching down to an InGaAs etch stop layer. This leaves us with a wafer containing the silicon waveguides and the III-V active layer in which the amplifier mesas can be defined using standard wafer scale processes, lithographically aligned to the underlying SOI waveguide circuit. A Ti/Pt/Au stripe, acting as a p-side contact and also as a hard mask for the mesa etching was defined with a lift-off process using 320 nm UV contact lithography. Selective wet etching was used to etch through the InGaAs layer, the InP p-doped layer and the MQW. By carefully selecting the orientation of the amplifier mesa with respect to the crystal orientation, a negative sidewall slope can be achieved in the anisotropic etching of InP. GeAu/Ni was used for the n-contacts. The active waveguide is encapsulated with DVS-BCB and extra Ti/Au contacts layers were added for the contact pads. The microscope pictures in Fig. 2 were taken before the final metallization and clearly show the amplifier mesas and the n-type metallization. Using the fabrication process outlined above a taper width of 500 nm, required for low loss coupling, is reliably obtained even though it relies on standard contact mask lithography.

4. Measurement results

4.1 Characterization of passive demultiplexers

As a first step, we characterized the performance of the passive demultiplexers. The spectral response of the ring resonators was measured using the amplifiers in reverse bias as integrated detectors. Light from an external tunable laser was coupled in the chip through the grating

#187534 - $15.00 USD Received 21 Mar 2013; revised 6 May 2013; accepted 7 May 2013; published 30 May 2013

coupler and after passing through the ring resonator detected in the reversely biased SOA's. Figure 3(a) shows the result. The measured channel bandwidth was 25 GHz, which is better than the design value, while the average channel spacing (250 GHz) and the FSR (17 nm) are very close to the design values. The insertion loss of the ring is estimated to be 1 dB. The AWG-devices were characterized by forward biasing the SOA's and measuring the amplified spontaneous emission using an optical spectrum analyzer (0.1 nm resolution bandwidth) through two extra waveguides connected at the output side of the AWG and not terminated with a DBR mirror (Fig. 3(b)). We found a channel spacing of 200 GHz, a channel bandwidth of 89.66 GHz and a FSR of 35 nm for the AWG, all very close to the design values. The AWG excess loss was estimated to be 2.5 dB.

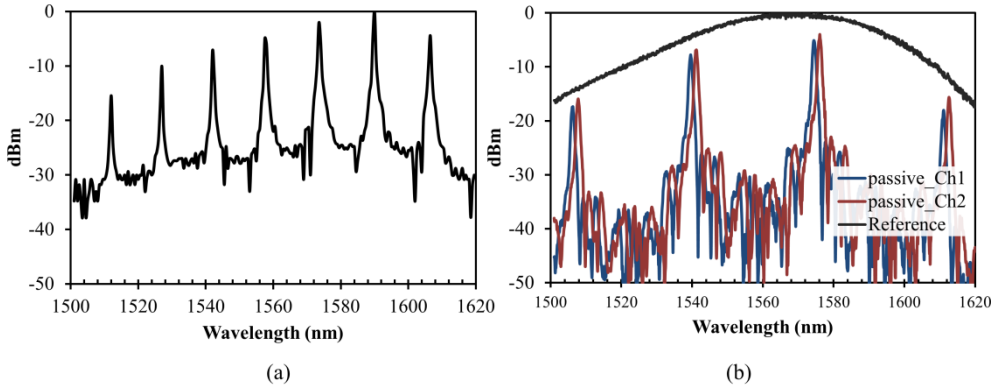

Fig. 3. (a) Filter characteristic for ring resonator demultiplexer measured using a tunable laser and the SOA as detector. The curve is normalized to its maximum and contains the response of the ring resonator itself, the DBR-front mirror and a focusing grating coupler. (b) Filter characteristic of the AWG by measuring the ASE from the SOA's filtered through the device. The black curve shows the response of the fiber-to-chip grating coupler. The blue and red curves show the response of two neighboring AWG-channels and the grating coupler.

4.2 Characterization of ring-based MFL

All devices were characterized on a temperature controlled stage at 20°C. Figure 4(a) shows the LI and VI-curves for all 4 channels of the RMFL. The threshold current and slope efficiency vary from 31 mA to 39 mA and 37.5 mW/A to 30 mW/A respectively. An output power of more than 1 mW in the silicon waveguide is obtained. The series resistance is 6 Ohm. Figure 4(b) shows the superimposed spectra of all 4 channels, with the amplifiers biased at 55 mA. As expected from the narrow filter bandwidth provided by the ring resonators, stable single mode lasing is obtained (see high-resolution spectra in the inset of Fig. 4(b). In addition, for these pumping conditions the spectra exhibit a side mode suppression of 45 dB with respect to the modes in other passbands. However, in some cases lasing in multiple passbands is obtained, related to the relatively small FSR of the ring resonators. To avoid this, the FSR has to be increased or an additional intra-cavity filter has to be included, e.g. by tailoring the DBR-mirrors as discussed above.

#187534 - $15.00 USD Received 21 Mar 2013; revised 6 May 2013; accepted 7 May 2013; published 30 May 2013

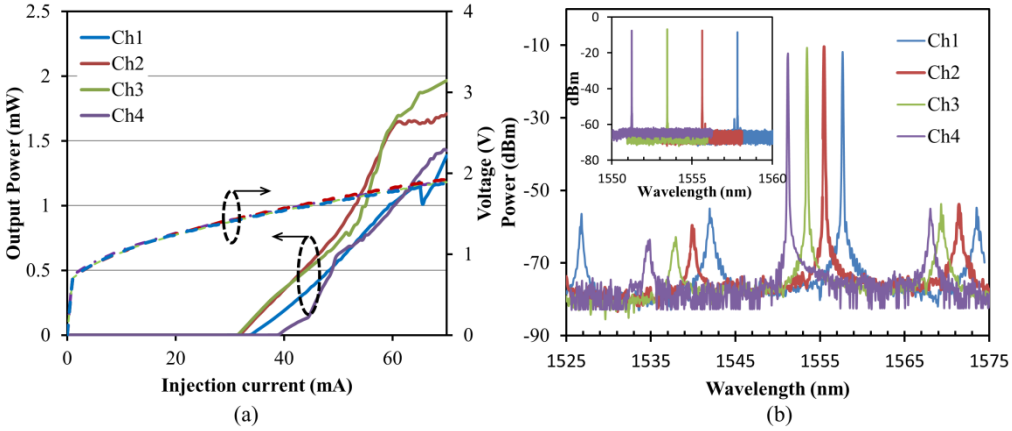

Fig. 4. a) LIV curves for the ring based demultiplexer. The output power refers to the amount of light coupled in the silicon waveguide b) Superimposed spectra for the 4 channels (resolution bandwidth 0.1 nm). The inset shows the spectra measured with a resolution bandwidth of 0.2 pm.

Figure 5(a) shows the LI-curves for different stage temperatures, for channel 2 of the RMFL. Lasing up to at least 60°C is obtained and up to 7 mW waveguide coupled power is obtained at 10 °C. The characteristic temperature T_0 of the laser is 100 K.

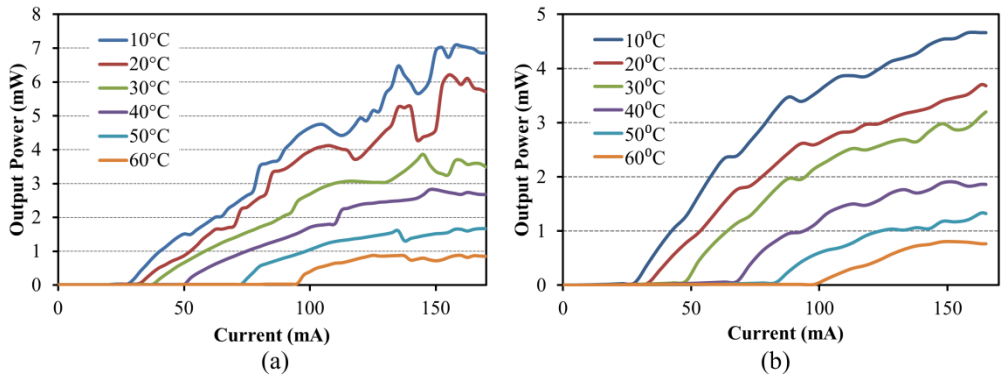

Fig. 5. Output power as a function of current for different stage temperatures for the RMFL (a) and AMFL (b). Lasing up to temperatures of 60°C is obtained in both cases.

Figure 6 shows the line width of channel 2 as a function of output power, measured through a delayed-self heterodyne method [12], using an 80 MHz modulation and using 22.5 km of single mode fiber. The line shape of the beat signal is measured on an RF spectrum analyzer with a 10 kHz resolution bandwidth. The passive external cavity and the relatively high intra-cavity power ensure a line width of less then 1.5 MHz at injection currents above 55 mA.

#187534 - $15.00 USD Received 21 Mar 2013; revised 6 May 2013; accepted 7 May 2013; published 30 May 2013

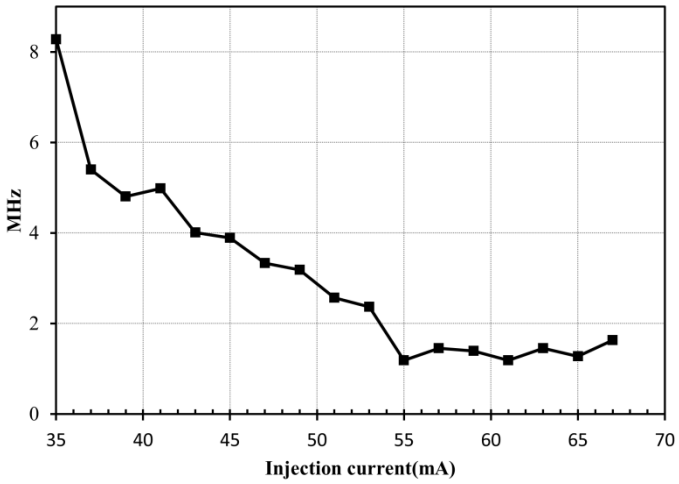

Fig. 6. Linewidth measurement of the ring-resonator based multi-frequency laser

4.3 Characterization of AWG-based MFL

Figure 7(a) shows the LI-curves for all 4 channels of the AMFL. One channel had a damaged taper tip and exhibits a considerably higher threshold current. For the other channels the threshold current varies from 32 mA to 42 mA. An output power of over 3 mW (in the silicon waveguide) is obtained for the good channels. Figure 5(b) shows the temperature dependence of the output power characteristics for channel 2 of the AMFL, which is similar to that of the RMFL (lasing up to 60°C, characteristic temperature T0 = 95 K).

From the superimposed spectra shown in Fig. 7(b) it is immediately obvious that lasing in lower and higher passbands is suppressed strongly in this case, which is related to the large FSR of the AWG. Measurements using a high-resolution optical spectrometer (Apex Technologies AP2041A) shown in the inset of Fig. 7(b) resolve the different longitudinal modes around the main mode (measured mode spacing 15 GHz). Despite the larger channel bandwidth also this device is clearly lasing in a single longitudinal mode. Line width measurements show similar values as for the RMFL (1.2 MHz at 80 mA)

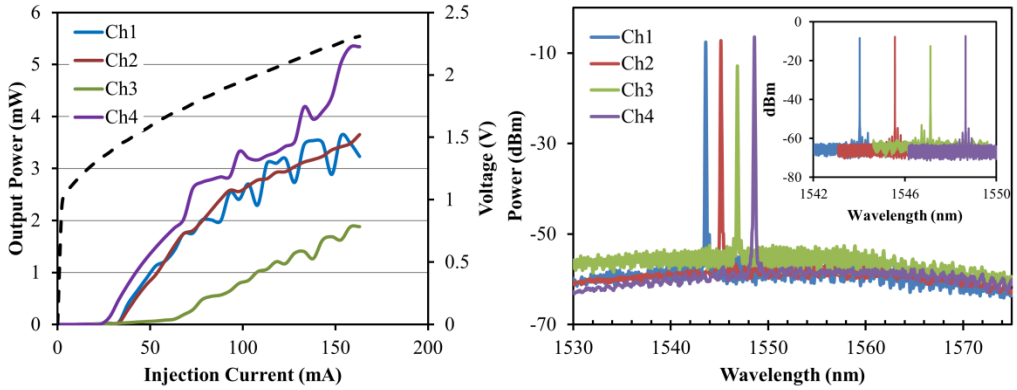

Fig. 7. a) LIV curves for the ring based demultiplexer. The output power refers to the amount of light coupled in the silicon waveguide b) Superimposed spectra for the 4 channels (resolution bandwidth 0.1 nm). The inset shows the spectra measured with a resolution bandwidth of 0.2 pm.

#187534 - $15.00 USD Received 21 Mar 2013; revised 6 May 2013; accepted 7 May 2013; published 30 May 2013

6. Conclusion

We demonstrated two types of multi-frequency lasers, respectively based on an AWG and ring resonator intra-cavity demultiplexer. Threshold currents between 30 and 40 mA and output powers up to 7 mW were obtained. The combined effect of the intra-cavity filter and four wave mixing ensures strong suppression of longitudinal modes nearby the lasing mode [8] resulting in a side mode suppression of over 45 dB. The relatively small FSR of the ring resonators cannot fully avoid mode hopping to lower pass bands of the device however. This effect is not present in the AWG based MFL, were lasing in neighboring passbands is completely suppressed. This work demonstrates the versatility of the heterogeneous integration process we developed. The short bending radius provided by the silicon waveguide platform results in very compact demultiplexer devices and a cavity length which is considerably smaller than that of most MFL devices published before. This makes these devices promising candidates for applications in need of direct modulation or high speed digital wavelength switching.

Acknowledgments

We acknowledge support of the EU through the ICT-HELIOS project and the ERC-ULPPIC project.

#187534 - $15.00 USD Received 21 Mar 2013; revised 6 May 2013; accepted 7 May 2013; published 30 May 2013